



## In vivo biocompatibility of a new hydrophobic coated Al/Al<sub>2</sub>O<sub>3</sub> nanowire surface on stents



Axel Rentzsch<sup>a,\*</sup>, Eva Metz<sup>a</sup>, Ruben Mühl-Benninghaus<sup>b</sup>, Alexander Maßmann<sup>c</sup>, Stephanie Bettink<sup>d</sup>, Bruno Scheller<sup>d</sup>, Lilia Lemke<sup>a,h</sup>, Ali Awadelkareem<sup>a</sup>, Toshiki Tomori<sup>b</sup>, Ayman Haidar<sup>a</sup>, Matthias W. Laschke<sup>e</sup>, Michael D. Menger<sup>e</sup>, Cenk Aktas<sup>g</sup>, Matthias Hannig<sup>h</sup>, Norbert Pütz<sup>h</sup>, Thomas Büttner<sup>i</sup>, David Scheschkewitz<sup>i</sup>, Michael Veith<sup>f,i</sup>, Hashim Abdul-Khaliq<sup>a</sup>

<sup>a</sup> Clinic for Pediatric Cardiology, Saarland University Hospital, Homburg, Saar, Germany

<sup>b</sup> Department of Neuroradiology, Saarland University Hospital, Homburg, Saar, Germany

<sup>c</sup> Department of Radiology and Nuclear Imaging, Robert Bosch Hospital, Stuttgart, Germany

<sup>d</sup> Clinical and Experimental Interventional Cardiology, Saarland University Hospital, Homburg, Saar, Germany

<sup>e</sup> Institute for Clinical and Experimental Surgery, Saarland University Hospital, Homburg, Saar, Germany

<sup>f</sup> INM – Leibniz Institute for New Materials, Campus D2 2, Saarbrücken, Germany

<sup>g</sup> Institute for Materials Science, Faculty of Engineering, Christian-Albrechts-University of Kiel, Kiel, Germany

<sup>h</sup> Clinic of Operative Dentistry, Periodontology and Preventive Dentistry, Saarland University Hospital, Homburg, Saar, Germany

<sup>i</sup> General and Inorganic Chemistry, Saarland University, Saarbrücken, Germany

### ARTICLE INFO

#### Keywords:

In-stent restenosis

Bare metal stent

Innovation

Optical coherence tomography

### ABSTRACT

**Background:** Intima proliferation and in-stent restenosis is a challenging situation in interventional treatment of small vessel obstruction. Al/Al<sub>2</sub>O<sub>3</sub> nanowires have been shown to accelerate vascular endothelial cell proliferation and migration in vitro, while suppressing vascular smooth muscle cell growth. Moreover, surface modification of Al/Al<sub>2</sub>O<sub>3</sub> nanowires with poly[bis(2,2,2-trifluoromethoxy)phosphazene (PTFEP) coating enables further advantages such as reduced platelet adhesion. Therefore, the study's goal was to compare the biocompatibility of novel Al/Al<sub>2</sub>O<sub>3</sub> + PTFEP coated nanowire bare-metal stents to uncoated control stents in vivo using optical coherence tomography (OCT), quantitative angiography and histomorphometric assessment.

**Methods:** 15 Al/Al<sub>2</sub>O<sub>3</sub> + PTFEP coated and 19 control stents were implanted in the cervical arteries of 9 Aachen minipigs. After 90 days, in-stent stenosis, thrombogenicity, and inflammatory response were assessed. Scanning electron microscopy was used to analyse the stent surface.

**Results:** OCT analysis revealed that neointimal proliferation in Al/Al<sub>2</sub>O<sub>3</sub> + PTFEP coated stents was significantly reduced compared to control stents. The neointimal area was  $1.16 \pm 0.77 \text{ mm}^2$  in Al/Al<sub>2</sub>O<sub>3</sub> + PTFEP coated stents vs.  $1.98 \pm 1.04 \text{ mm}^2$  in control stents ( $p = 0.004$ ), and the neointimal thickness was  $0.28 \pm 0.20$  vs.  $0.47 \pm 0.10$  ( $p = 0.003$ ). Quantitative angiography showed a tendency to less neointimal growth in coated stents. Histomorphometry showed no significant difference between the two groups and revealed an apparent inflammatory reaction surrounding the stent struts.

**Conclusions:** At long-term follow-up, Al/Al<sub>2</sub>O<sub>3</sub> + PTFEP coated stents placed in peripheral arteries demonstrated good tolerance with no treatment-associated vascular obstruction and reduced in-stent restenosis in OCT. These preliminary in vivo findings indicate that Al/Al<sub>2</sub>O<sub>3</sub> + PTFEP coated nanowire stents may have translational potential to be used for the prevention of in-stent restenosis.

### 1. Introduction

Over the last 30 years, interventional cardiology has evolved into a critical component in treating congenital heart defects, both curative and palliative. Even in small children, heart operations can be replaced or

postponed [1]. The structure of implants used in minimally invasive procedures is becoming more precise, smaller, and diverse [2]. However, the implantation of small stents into still-growing blood vessels in children is hampered by in-stent restenosis caused by intimal proliferation and complicated by thrombotic stent obstruction [3]. In-stent restenosis is caused

\* Corresponding author at: Clinic for Pediatric Cardiology, Saarland University Hospital, Kirrberger Str. 100, 66421 Homburg, Saar, Germany.  
E-mail address: [axel.rentzsch@uks.eu](mailto:axel.rentzsch@uks.eu) (A. Rentzsch).

by a complex interaction between endothelial cells, smooth muscle cells (SMC), platelets, and inflammatory cells, which results in excessive proliferation of SMC and narrowing of the vascular lumen [4]. The threat of drug-eluting stents is an uncontrolled, potentially toxic release of the drug in young children [5]. In addition, specifically coated stents for pediatric procedures such as pulmonary artery stents (e.g., for pulmonary atresia, hypoplastic pulmonary arteries), pulmonary vein stents, or ductal stenting are not commercially available.

As a result of extensive research in recent years, the study group has developed different nanostructured surfaces, which exhibit anti-thrombotic and anti-inflammatory properties [6]. Metal/metal oxide heterostructures with core-shell hierarchy demonstrated new functional properties when compared to their constituent compounds [7]. It is well established that modified surfaces may promote more cell adhesion when compared to untreated surfaces [8]. In a previous study, we found that laser treatment reduces myofibroblast proliferation while not affecting endothelial cell proliferation [9]. There are numerous effects of micro- and nanoscale alumina surface topographies on cellular function, adhesion, proliferation, and gene regulation [10,11]. The impact of nano-topography on cell-surface interaction is critical for the advancement of stent material design. For instance, we demonstrated that, in terms of topography-driven cell response, human umbilical vein endothelial cells preferentially adhere on Al/Al<sub>2</sub>O<sub>3</sub> nanowires, whereas growth of human umbilical vein SMC is suppressed [12].

The addition of a polymer coating (poly[bis(2,2,2-trifluoromethoxy) phosphazene], PTFEP) to the surface of Al/Al<sub>2</sub>O<sub>3</sub> nanowires resulted in ultra-hydrophobic properties without altering the nanostructured surface topography [13]. Furthermore, it could be demonstrated that the modified surface has a high repellence to blood. Platelet adhesion and activation were significantly reduced, as was bacterial adherence, and there was no cytotoxic effect on vascular cells [6]. Based on these promising findings, the Al/Al<sub>2</sub>O<sub>3</sub> nanowire surface with PTFEP coating has already been patented by the German Patent and Trade Mark Office [14]. Fig. 1 chronologically summarizes the major steps in the development of Al/Al<sub>2</sub>O<sub>3</sub> coated stents with PTFEP coating.

Stents with Al/Al<sub>2</sub>O<sub>3</sub> nanowire coating and super-hydrophobic PTFEP surface are expected to induce less pronounced neointimal proliferation resulting in in-stent restenosis than conventional stents. To test this hypothesis, we compared the development of neointima in Al/Al<sub>2</sub>O<sub>3</sub> + PTFEP coated stents to bare metal stents in vivo using optical coherence tomography (OCT), quantitative angiography, and histomorphometry.

## 2. Methods

### 2.1. Stent preparation

The Al/Al<sub>2</sub>O<sub>3</sub> precursor preparation and coating of bare-metal stents have previously been described in detail [7,11]. An overview of the technical details is presented in Supplement 1. Light microscopic quality control of all Al/Al<sub>2</sub>O<sub>3</sub> + PTFEP coated stents was performed, after which the stents with the best-performing coating without cracks or interruptions were selected for the in vivo experiment.

### 2.2. Animals

Animal experiments were carried out in nine female Aachen minipigs aged 18 to 24 months, weighing 70 to 92 kg. The animals were purchased from a farm specialized in breeding Aachen minipigs. The study protocol was reviewed and approved by the federal authority (approval ID: 09/2019) for compliance with the national animal welfare act. It was carried out in accordance with the European animal protection legislation (Directive 2010/63/EU). All experiments were performed at the Institute for Clinical and Experimental Surgery, Saarland University, Germany.

### 2.3. Animal procedure

All animals received a one-day pre-treatment with 200 mg acetylsalicylic acid. Intramuscular injections of xylazine (2.5 mg/kg body weight), ketamine (30 mg/kg body weight) and atropine (1 mg) were used to induce sedation. Subsequently, the animals were placed in a stable supine position after being transferred to the operating room. An intravenous line with 0.9 % saline solution was set up for intraoperative fluid supply. For analgesia, carprofen (4 mg/kg body weight) was administered intravenously to the animals at the start and end of the procedure. After orotracheal intubation inhalative isoflurane (2–3 %) was used to maintain anaesthesia. A 6 French introducer sheath was inserted into the femoral artery using ultrasound guidance followed by heparin administration of 100 IU/kg body weight. Cervical target vessels (A. cervicalis interna, A. carotis externa) of appropriate size for stent implantation were angiographically selected. These vessels were selected to ensure the easiest possible stent implantation with minimal curvature and without dislocation. Al/Al<sub>2</sub>O<sub>3</sub> + PTFEP coated stents were manually crimped on balloon catheters

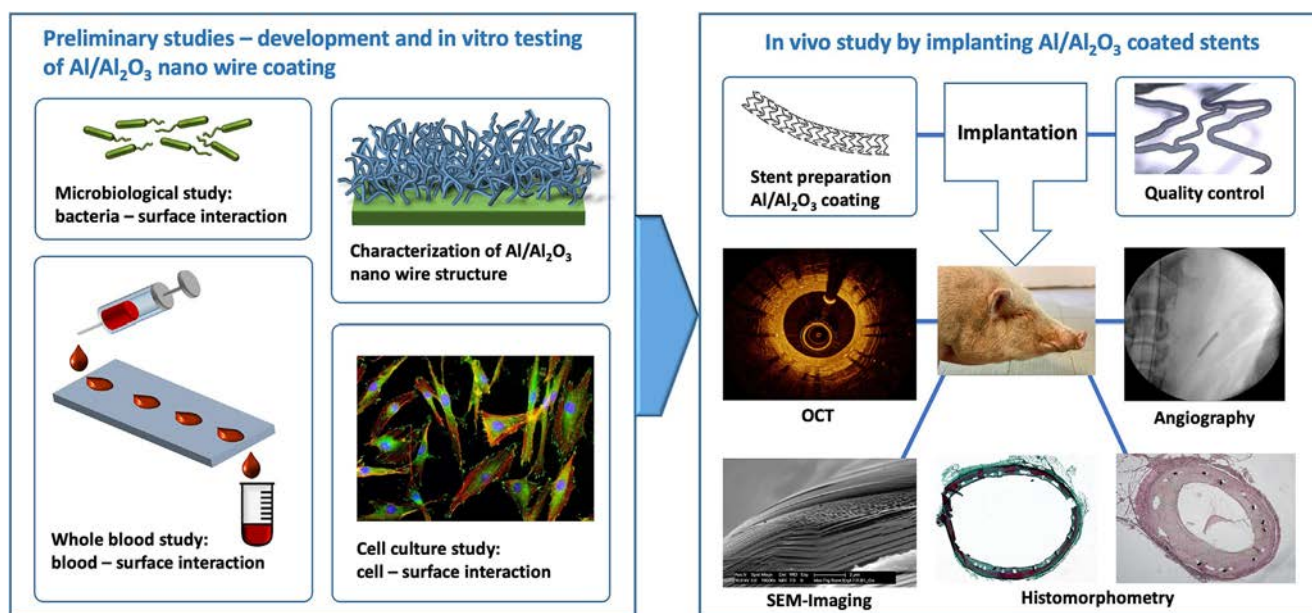


Fig. 1. The overview summarizes the major milestones in the development of biocompatible Al/Al<sub>2</sub>O<sub>3</sub> + PTFEP coated stents, which progressed from surface characterization to microbiological and cell interaction studies, intending to create a prototype biocompatible stent surface that can be used in animal models.

of appropriate size of the same manufacturer before being implanted in the target vessel in a non-curved segment. Commercially available cobalt-chromium L-605 (Coroflex stents) and stainless steel 316-L (Cordis stents, ZETA stents) bare-metal stents were implanted as control stents. For 20 s, a stent-to-artery ratio of 1,3:1 was used for stent dilation. Fifteen Al/Al<sub>2</sub>O<sub>3</sub> + PTFEP coated stents and nineteen control stents were implanted in total. Each Al/Al<sub>2</sub>O<sub>3</sub> + PTFEP coated stent was implanted proximal to a control stent in the same vessel, and four control stents were implanted individually in a vessel. Stent diameters ranged from 3 to 4 mm and lengths from 8 to 24 mm. Until sacrifice, all animals received daily oral doses of 100 mg acetylsalicylic acid and 75 mg clopidogrel.

All animals were subjected to control angiography and OCT acquisition after 90 days. Thereafter, 3 to 6 g sodium pentobarbital was used to euthanize the animals. The stents were surgically removed and embedded in a 4 % formalin solution.

#### 2.4. Quantitative angiography

A monoplane fluoroscopic system was used to acquire angiographic imaging (Ziehm Vision imaging, Nuremberg, Germany). As a contrast agent, Bracco Imaging's Solustrast 300 (Milan, Italy) was used. The following parameters were assessed: Reference vessel diameter, stent diameter and overstretch ratio at baseline, minimal luminal diameter and late loss at the 90-day follow-up angiography. Late loss was calculated as the difference between luminal diameter at implantation minus minimal luminal diameter after 90 days.

#### 2.5. Optical coherence tomography

A 6 French guiding catheter and a 0.014-inch wire were used to place a 2.7 F Dragonfly OPTIS imaging catheter (St. Jude Medical/Abbott Laboratories, Illinois, USA) in the target vessel for OCT image acquisition. The imaging lens at the tip of the catheter was positioned 10 mm behind the distal stent under fluoroscopy. The vessel was manually flushed with 10 ml of contrast media, and images were captured with a high temporal resolution of 180 frames/s while the imaging catheter was automatically pulled back at 18 mm/s. OCT images were analysed offline by an experienced radiologist blinded to the histomorphometric results. The proximal, medial, and distal segments of each stent were measured. The cross-section with the highest degree of stenosis in each stent third was selected for measurement. Mean stent area (mm<sup>2</sup>) and mean luminal area (mm<sup>2</sup>) were measured and mean neointimal area (mm<sup>2</sup>) was calculated by subtracting luminal area from stent area. The mean area obstruction was calculated by dividing the neointimal area by the stent area\*100 (in %). The distance from the inner stent surface to the luminal border was used to calculate mean neointimal thickness (NIT).

#### 2.6. Histologic and morphologic analysis

Under constant agitation, the formalin-fixed specimens were cleaned of extraneous fatty tissue residues and dehydrated with ethanol and xylene. After that, the specimens were immersed in methyl methacrylate (MMA). The MMA vessel blocks were cut at four points with a cutting microtome (diamond knife), and several 10–12 μm thick sections were made in each case. Final specimens were stained by hematoxylin and eosin and Masson-Goldner technique. Each stent had approximately 15 sections taken, the section with the highest quality of each stent third (distal, medial, and proximal) was examined. Histomorphometric measurements were performed using specialized imaging software (LUCIA G 5.00). The external elastic lamina (EEL), internal elastic lamina (IEL), and lumen area were all semi-automatically bypassed, and the neointima area (NA) was calculated as the difference between the IEL and the lumen area. The area of obstruction was calculated as NA/IEL\*100 (in %). The thickness of the neointima was measured from the lumen to the IEL or endoluminal stent site. Mean neointimal thickness was measured at 10–12 sites around the circumference and averaged. The injury and inflammation scores

were calculated in the manner described previously by Schwartz [15]. Fibrin score was assessed based on Moreno et al. [16] as follows: (0) No fibrin deposition around strut, (1) fibrin deposition in <25 % around the strut, (2) fibrin deposition 25–50 % around strut, (3) fibrin deposition 50–75 % around strut, (4) fibrin deposition 100 % around strut.

Scanning electron microscopic (SEM) imaging was performed on one Al/Al<sub>2</sub>O<sub>3</sub> + PTFEP coated stent and one control stent that had been embedded in polymethyl methacrylate (PMMA). For SEM analysis, samples were sputter-coated with carbon. SEM analysis was carried out using an XL30 ESEM FEG (FEI, Eindhoven, The Netherlands) at 5 kV and 10 kV, respectively, at up to 20,000-fold magnification. Additionally, an energy dispersive X-ray analysis (EDX) was performed.

#### 2.7. Statistical analysis

As the parameters of the histomorphometric analysis and OCT had a roughly Gaussian shape in a graphical check by boxplots, they were reported as means and standard deviations and compared between Al/Al<sub>2</sub>O<sub>3</sub> + PTFEP coated stents and uncoated stents using the Student's *t*-test in the version for different variances. Pearson's correlation coefficient was used to investigate the relationship between variables and a test for the null hypothesis of independence. SPSS 17.0 and MS Excel Version 16.68 were used for computations. *P* values <0.05 were considered significant.

### 3. Results

Fifteen Al/Al<sub>2</sub>O<sub>3</sub> + PTFEP coated stents and nineteen control stents (8 stents 316-L stainless steel, 11 stents cobalt-chromium L-605) were initially implanted. In two vessels, the proximal control stent migrated into the distal Al/Al<sub>2</sub>O<sub>3</sub> + PTFEP coated stent in the same vessel, resulting in a stent-in-stent configuration. These stents were excluded from the analysis. One Al/Al<sub>2</sub>O<sub>3</sub> + PTFEP coated and six control stents could not be located at explantation. Visual examination of the explanted stents revealed no evidence of acute thrombosis or arterial occlusion. During dissection, no thrombus was visible through the visible stent struts. Finally, the histological analysis included 12 Al/Al<sub>2</sub>O<sub>3</sub> + PTFEP coated and 11 control stents.

#### 3.1. Quantitative angiography

Stent sites were angiogrammed before and after stent implantation and at the 90-day follow-up, which was feasible for 12 Al/Al<sub>2</sub>O<sub>3</sub> + PTFEP coated stents and 17 control stents. This confirmed the correct position of the stents. Quantitative angiography further revealed that the two groups agreed on reference vessel diameter, stent diameter, and overstretch ratio. At the 90-day follow-up the minimal luminal diameter was larger in Al/Al<sub>2</sub>O<sub>3</sub> + PTFEP coated stents and late loss was reduced, indicating a less pronounced neointimal growth in Al/Al<sub>2</sub>O<sub>3</sub> + PTFEP coated stents; however, values did not reach statistical significance (Table 1). There was

**Table 1**

Quantitative angiography of cervical arteries at implantation and 90-day follow-up. Overstretch ratio = stent diameter/reference vessel diameter\*100, late loss = luminal diameter at implantation minus minimal luminal diameter after 90 days. Data presented as mean ± SD.

	Al/Al <sub>2</sub> O <sub>3</sub> + PTFEP coated stents (n = 12)	Control stents (n = 17)	p
Quantitative angiography at stent implantation			
Reference vessel diameter (mm)	1.95 ± 0.46	1.95 ± 0.50	0.98
Stent diameter (mm)	2.48 ± 0.38	2.60 ± 0.70	0.63
Overstretch ratio (%)	132.3 ± 33.4	128.5 ± 18.4	0.74
Quantitative angiography at 90-day follow-up			
Minimal luminal diameter (mm)	2.07 ± 0.52	1.82 ± 0.27	0.29
Late loss (mm)	0.45 ± 0.39	0.62 ± 0.25	0.37

**Table 2**

OCT findings of stented cervical arteries at 90-day follow-up. Mean area obstruction calculated at all measured sites as neointimal area/stent area\*100. Data presented as mean  $\pm$  SD.

	Al/Al <sub>2</sub> O <sub>3</sub> + PTFEP coated stents	Control stents	p
n (analysed stents)	8	9	
Mean luminal area (mm <sup>2</sup> )	5.23 $\pm$ 2.61	4.91 $\pm$ 2.08	0.80
Mean stent area (mm <sup>2</sup> )	6.41 $\pm$ 2.66	6.92 $\pm$ 2.73	0.72
Mean neointimal area (mm <sup>2</sup> )	1.16 $\pm$ 0.77	1.98 $\pm$ 1.04	0.004
Mean area obstruction (%)	20.17 $\pm$ 11.02	29.80 $\pm$ 10.35	0.006
Area obstruction distal (%)	16.51 $\pm$ 9.67	25.99 $\pm$ 6.22	0.05
Area obstruction medial (%)	20.42 $\pm$ 13.02	29.82 $\pm$ 13.66	0.19
Area obstruction proximal (%)	21.71 $\pm$ 13.03	31.35 $\pm$ 10.15	0.14
Mean neointimal thickness (mm)	0.28 $\pm$ 0.20	0.47 $\pm$ 0.19	0.003
Neointimal thickness distal (mm)	0.20 $\pm$ 0.12	0.41 $\pm$ 0.15	0.02
Neointimal thickness medial (mm)	0.31 $\pm$ 0.20	0.49 $\pm$ 0.23	0.13
Neointimal thickness proximal (mm)	0.34 $\pm$ 0.23	0.51 $\pm$ 0.17	0.15

no thrombus deposition in either the Al/Al<sub>2</sub>O<sub>3</sub> + PTFEP-coated or control stents.

### 3.2. OCT analysis

OCT images were available for eight Al/Al<sub>2</sub>O<sub>3</sub> + PTFEP coated stents and nine control stents. Table 2 summarizes the findings of the OCT analyses. Intraluminal thrombus formation was not observed, and all vessels were seen open with no vessel obstruction. The mean neointimal area was 1.16  $\pm$  0.77 mm<sup>2</sup> in Al/Al<sub>2</sub>O<sub>3</sub> + PTFEP coated stents and 1.98  $\pm$  1.04 mm<sup>2</sup> in control stents ( $p = 0.004$ ). The mean area obstruction ( $p = 0.006$ ) and the mean neointimal thickness ( $p = 0.003$ ) were significantly reduced in Al/Al<sub>2</sub>O<sub>3</sub> + PTFEP coated stents compared to control stents. By OCT, no significant differences were seen between 316 L and L-305

**Table 3**

Histomorphometric results of explanted Al/Al<sub>2</sub>O<sub>3</sub> + PTFEP coated and control stents at 90-day follow-up. EEL external elastic lamina, IEL internal elastic lamina, NA neointima area (= IEL area minus lumen area). Data presented as mean  $\pm$  SD.

	Al/Al <sub>2</sub> O <sub>3</sub> + PTFEP coated stents	Control stents	p
n (analysed stents)	12	11	
EEL area (mm <sup>2</sup> )	7.90 $\pm$ 3.23	8.78 $\pm$ 6.47	0.53
IEL area (mm <sup>2</sup> )	6.05 $\pm$ 2.64	6.85 $\pm$ 5.44	0.64
Lumen area (mm <sup>2</sup> )	2.80 $\pm$ 1.53	4.20 $\pm$ 4.88	0.16
NA (mm <sup>2</sup> )	2.85 $\pm$ 1.5	2.70 $\pm$ 1.66	0.81
Max. neointimal thickness (mm)	0.79 $\pm$ 0.43	0.70 $\pm$ 0.46	0.42
Mean neointimal thickness (mm)	0.45 $\pm$ 0.21	0.49 $\pm$ 0.28	0.54
Mean neointimal thickness distal	0.40 $\pm$ 0.20	0.44 $\pm$ 0.31	0.68
Mean neointimal thickness medial	0.43 $\pm$ 0.15	0.51 $\pm$ 0.28	0.47
Mean neointimal thickness proximal	0.53 $\pm$ 0.26	0.51 $\pm$ 0.25	0.88
Injury score	1.62 $\pm$ 0.78	1.36 $\pm$ 0.77	0.42
Inflammation score	1.96 $\pm$ 0.77	1.44 $\pm$ 0.93	0.16
Fibrin score	2.09 $\pm$ 0.79	1.84 $\pm$ 1.01	0.31

control stents. In all stents, the mean area obstruction and the mean neointimal thickness decreased from proximal to distal (Fig. 2).

### 3.3. Histomorphometric analysis

Histological examination revealed varying degrees of neointimal formation and lumen narrowing (Table 3, Fig. 3). There were no statistically significant differences between Al/Al<sub>2</sub>O<sub>3</sub> + PTFEP coated stents and control stents and between 316 L and L-605 control stents. Although the Al/Al<sub>2</sub>O<sub>3</sub> + PTFEP coated stents exhibited a slightly larger neointimal area, the mean neointimal thickness was lower in the Al/Al<sub>2</sub>O<sub>3</sub> + PTFEP coated stents, decreasing from proximal to distal, as seen on OCT. The stents in both groups experienced complete re-endothelialisation.

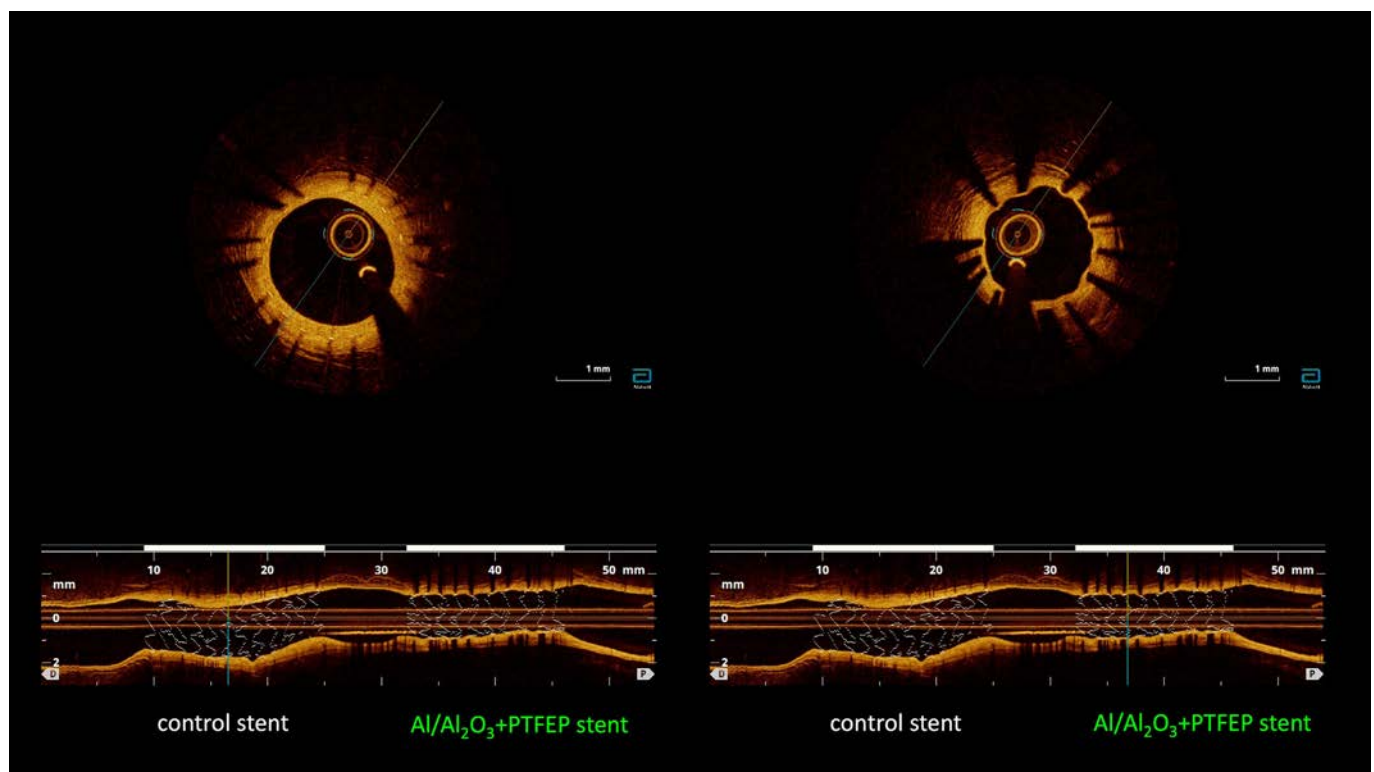


**Fig. 2.** Optical coherence tomography (OCT) cross-sectional view of a porcine cervical artery at 90-day follow-up. Cross-section through a control stent, top left; cross-section through an Al/Al<sub>2</sub>O<sub>3</sub> + PTFEP coated stent, top right. The reconstructed longitudinal vessel section in the lower image area shows the measurement points of the cross-sections. OCT shows neointimal formation in uncoated bare metal stents and suppression of neointimal proliferation in Al/Al<sub>2</sub>O<sub>3</sub> + PTFEP coated stents.

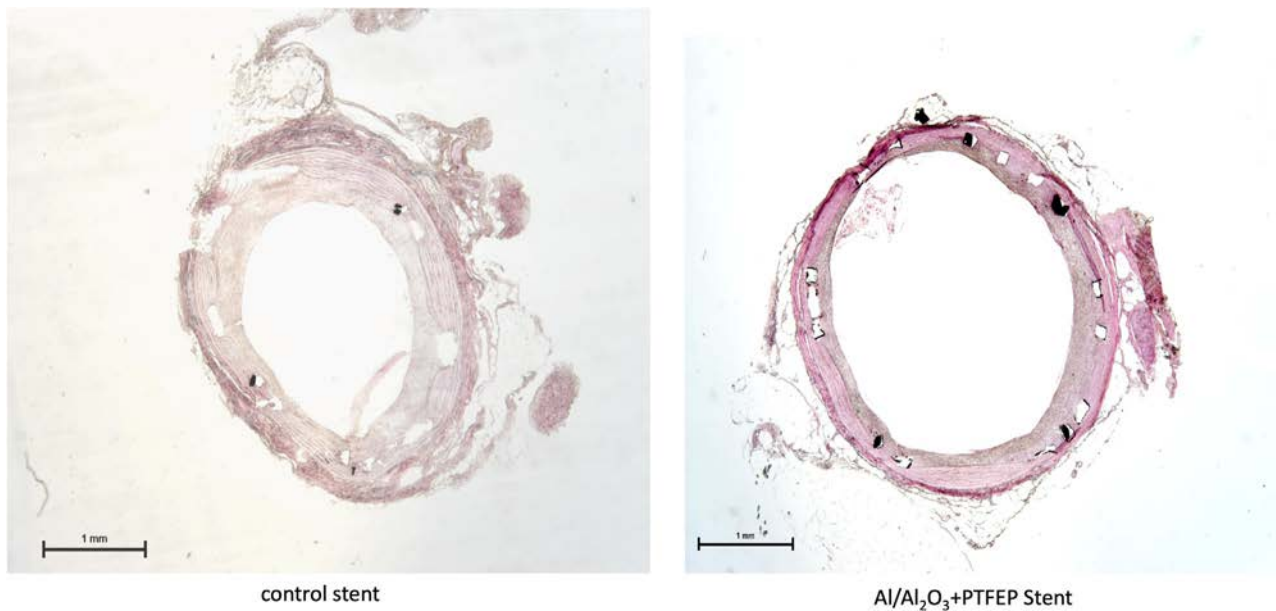


**Fig. 3.** Stented porcine cervical artery segment with neointimal formation in an Al/Al<sub>2</sub>O<sub>3</sub> + PTFEP coated stent (right) and bare metal stent (left) at 90-day follow-up (hematoxylin-eosin staining).

The assessed injury score indicated minor to moderate injury, which means that the internal elastic lamina was lacerated. The media was compressed, but the external elastic lamina was preserved. The extent of injury was comparable in both groups. The inflammation and fibrin scores did not differ significantly, though they were higher for the Al/Al<sub>2</sub>O<sub>3</sub> + PTFEP coated stents. There was a clear inflammatory response with cells surrounding the stent struts and increased fibrin deposition around coated stent struts (Fig. 4). The inflammation score correlated significantly with the maximum neointima thickness in both Al/Al<sub>2</sub>O<sub>3</sub> + PTFEP coated ( $r = 0.74$ ,  $p = 0.004$ ) and control stents ( $r = 0.61$ ,  $p = 0.035$ ).

### 3.4. SEM imaging

SEM imaging was used to visualize the coating on explanted stents. Fig. 5 shows the cross-section of an explanted Al/Al<sub>2</sub>O<sub>3</sub> + PTFEP coated stent. A distinctive layer is visible on the metal material of a stent cross

brace, indicating the Al/Al<sub>2</sub>O<sub>3</sub> + PTFEP coating (Fig. 5A, B). The specific nanowire structure as seen in Figure Suppl. is no longer visible, because it has been masked by proteins and cells. During the cutting procedure, the coating was detached and lifted from the stent surface, resulting in a gap between the stent and the layer, which elucidates the coating character of the structure on the stent. This intersection was used for energy dispersive X-Ray analysis (EDX, Fig. 5C, D). The performed EDX spectroscopy enables semi-quantitative analysis. Contamination from the environment, such as airborne components or from sample processing, can affect the chemical composition. Nevertheless, the EDX analysis allowed an unambiguous assignment of the components of the stents or their coating. The element composition of the stent showed high amounts of metallic components, including chromium (Cr: 15,2 % weight (wt)), nickel (Ni: 15,4 % wt) and iron (Fe: 59,5 % wt), indicating the stainless-steel alloy of the stent material. In comparison, the composition of the distinct coating layer (Fig. 5D) contained aluminium (Al: 7,6 % wt) as well as very high amounts of oxygen

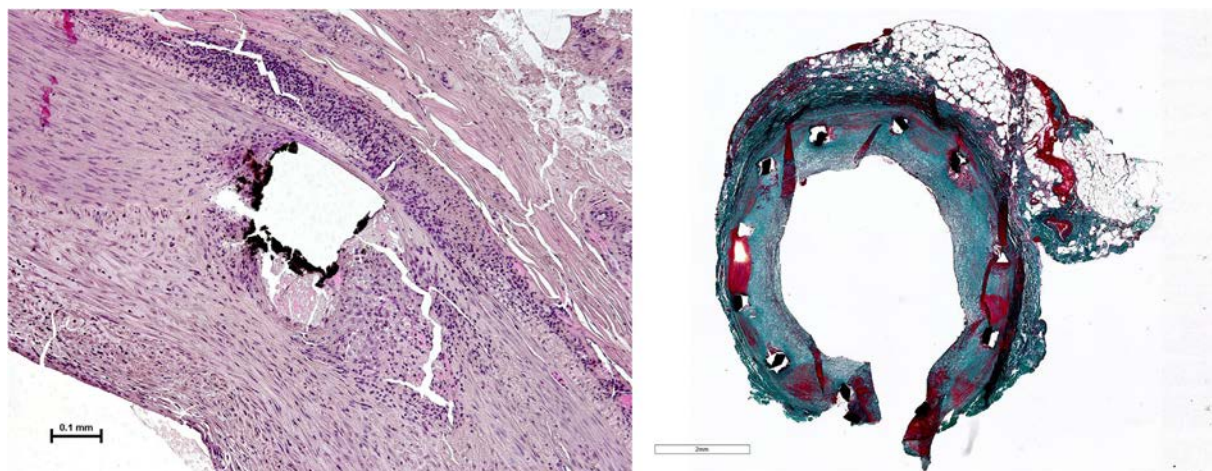


**Fig. 4.** Left: Inflammatory cells surrounding the Al/Al<sub>2</sub>O<sub>3</sub> + PTFEP coated stent strut in a vessel with pronounced neointimal growth (hematoxylin-eosin staining). Right: Masson Goldner staining with fibrin deposition (red) around all stent struts.

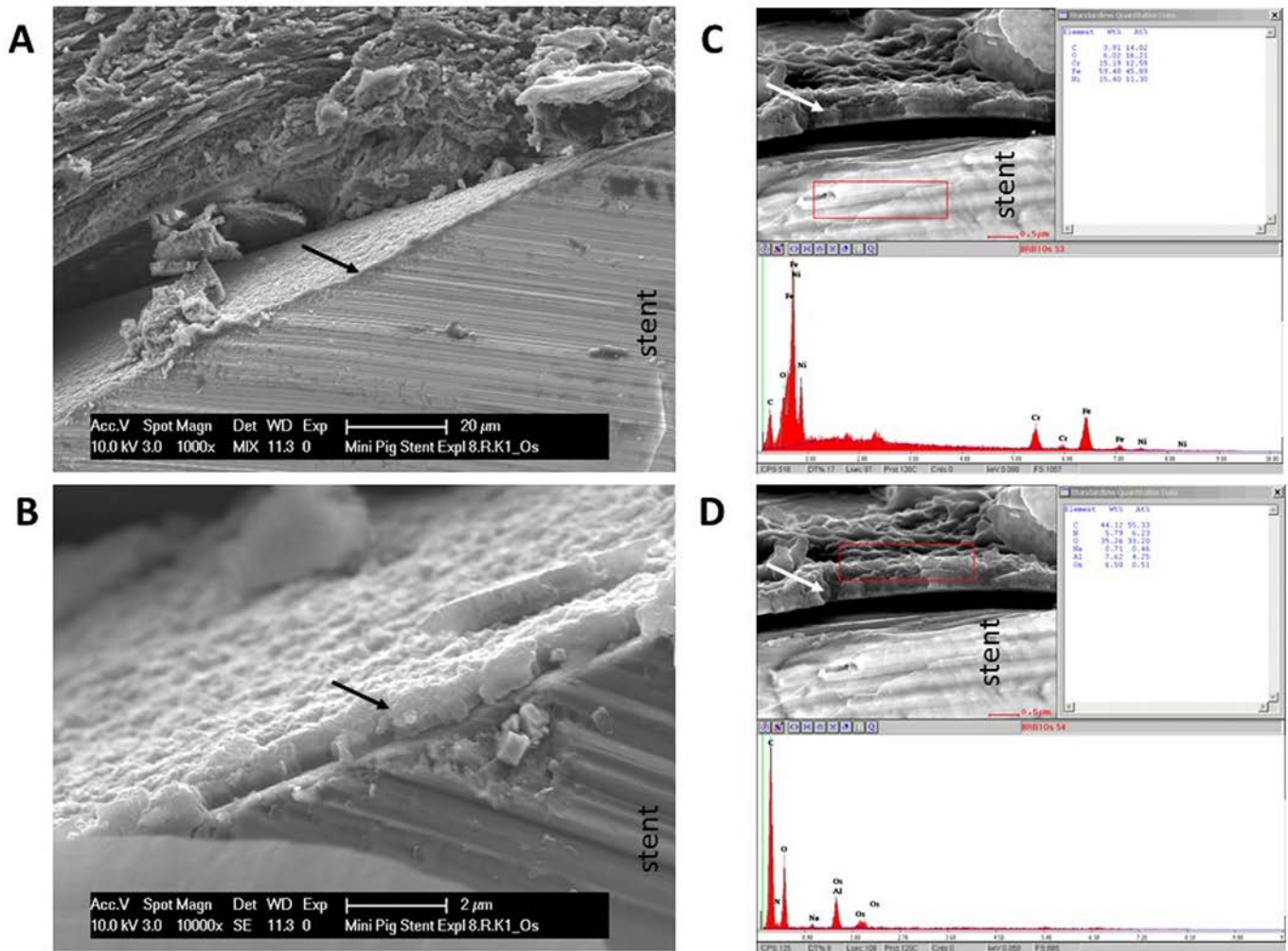


Fig. 5. SEM view of the cutting edge of an explanted Al/Al<sub>2</sub>O<sub>3</sub> + PTFEP coated stent at 1000× and 10,000× magnification (A, B). Arrows point to the Al/Al<sub>2</sub>O<sub>3</sub> + PTFEP coating. Energy-dispersive X-ray spectroscopy (EDX) analysis shows the composition of the constituents (C, D). Red squares indicate the exact position of EDX-analysis of the stent (C) and the coating (D) at 25000× magnification. The word “stent” indicates the front stent surface in the cross section.

(O: 35,3 % wt), suggesting the origin of both elements from the Al/Al<sub>2</sub>O<sub>3</sub> + PTFEP nanowire coating. A small quantity of oxygen was due to its reactivity and the rapid formation of an oxide layer on sample surfaces from the oxygen of the air, and could also be detected on bare metal. The presence of carbon in both areas is caused by the carbon sputter-coating procedure, which is essential for SEM analysis. The element osmium (Os: 6,5 % wt) was issued from the fixation solution containing osmium tetroxide.

#### 4. Discussion

Based on our previous results *in vitro* [6], we herein were able to bring the developed hybrid coating on complex three-dimensional surface structures and evaluated the cellular response to implanted stents in small peripheral vessels after 90 days. By this, we demonstrated that Al/Al<sub>2</sub>O<sub>3</sub> + PTFEP coated stents can be used *in vivo* safely and effectively with significantly lower intima proliferation and less in-stent stenosis in the OCT measurement. To our knowledge, this is the first experimental study to show a significant effect of this novel coating approach in small peripheral vessels.

Since intima proliferation in general presents the main challenging complication after stent implantation, we focused on its assessment using angiography, OCT and histomorphometry. In fact, we detected a significantly reduced formation of the neointimal cell layer in Al/Al<sub>2</sub>O<sub>3</sub> + PTFEP

coated stents compared to control bare metal stents by OCT 90 days after implantation. This reduction was true for all parts of the stents (proximal, medial, and distal). Previous studies have demonstrated that OCT is a reliable method with good agreement in terms of arterial healing when compared to light and electron microscopic results [17] as well as histologic examination [18] with excellent reproducibility [19]. A comparative study by Lemos et al. [20] showed very high agreement between intravascular ultrasound/OCT and histology, even though OCT uses stent area rather than IEL area. The reduced extent of neointimal cell growth supports our previous *in vitro* findings that an Al/Al<sub>2</sub>O<sub>3</sub> surface induces endothelialization while inhibiting SMC proliferation [12,21].

For the first time, a nanowire-coated stent surface was evaluated *in vivo* in the present study. However, *in vitro* studies with other metal oxide nanowire surfaces have already been conducted. They showed, for example, that nanowires of Co<sub>3</sub>O<sub>4</sub> exhibit an 11-day delay in drug release when compared to a flat cobalt-chrome substrate. This could be useful for drug-eluting implants that require a controlled release [22]. Although drug-eluting stents are not yet approved for pediatric cardiology, research has shown that ductal stenting with drug-eluting stents results in less luminal loss and fewer reinterventions [23]. In the field of percutaneous coronary interventions, the ultra-thin Orsiro sirolimus-eluting stent showed excellent long-term results compared to conventional drug-eluting stents in several randomised controlled trials [24,25]. It has a hybrid structure with a passive amorphous silicon carbide coating and a bioresorbable poly-L-lactide drug-eluting

coating. Although it does not take advantage of a nanostructured surface with ultrahydrophobic properties like Al/Al<sub>2</sub>O<sub>3</sub> + PTFEP coated stents, it shows antithrombogenic properties, induces little inflammation and shows early arterial healing [26]. Furthermore, after extensive in vitro studies on titanium dioxide there has been one in vivo study with TiO<sub>2</sub> nanotubular arrays on titanium stents that demonstrated excellent results in terms of neointimal cell growth and biocompatibility after implantation in iliofemoral rabbit arteries [27].

The OCT findings in our study, which were corroborated by quantitative angiography, showed clear differences between the Al/Al<sub>2</sub>O<sub>3</sub> + PTFEP coated stents and the control stents. However, histological examination revealed no clear significant differences between the two groups. These results can be explained by the two-dimensional cross-sectional assessment of histological samples. The qualitatively best section in each stent third was used for histologic evaluation. OCT assesses the whole stent-lumen before explantation and during perfusion, providing more representative information on the vessel wall and endothelial thickness within the implanted stent. Here, the section that best represents the stent third with the highest degree of stenosis was chosen for analysis. In consequence, the OCT results in our study may be more accurate in reflecting the amount of neointimal growth than the conventional histologic evaluation. In line with previous studies [18], we confirmed that OCT measurements of lumen and stent area are higher than corresponding values assessed by histologic measurements.

In other animal studies, the coating of stents with PTFEP alone without a nanostructured surface has been shown to reduce in-stent restenosis in peripheral and coronary arteries [28]. Such stents have also been used in humans for percutaneous coronary interventions with excellent results [29] in terms of clinical outcome and late lumen loss. According to our blood perfusion methods [6] we have previously demonstrated that only the synergistic effect of surface topography combined with the superior properties of PTFEP achieves a perfect biocompatible coating rather than nano structuring or PTFEP coating alone. Hence, Al/Al<sub>2</sub>O<sub>3</sub> + PTFEP coated stents are potential candidates for pediatric interventional practice, since in-stent stenosis may result in significant blood flow impairment after pediatric cardiac stent interventions [3].

Prevention of thrombus formation on cardiac devices is critical for clinical outcomes, especially after a vascular injury caused by implantation. Fluoropolymers have already been successfully used on materials in contact with blood, such as guide wires, vascular sutures, and vascular grafts, due to their anti-thrombotic and anti-inflammatory properties [30]. No thrombus formation was observed visually, angiographically, or by OCT in our study. This supports our preliminary findings [6] as well as other studies describing low thrombogenicity of PTFEP-covered stents in humans [29,30].

As measured by the inflammation score, the herein assessed number of inflammatory cells was comparable to that of common drug-eluting stents [31]. As demonstrated with a nanoporous stent coating of aluminium oxide ceramic material in swine, alumina itself may have pro-inflammatory properties. This showed a significantly increased inflammation score compared to bare metal stents. Though debris in the neointima can contribute [32], this was not found in the current study. On the contrary, a rabbit model showed that for Al/Al<sub>2</sub>O<sub>3</sub> ceramic surface alone and in combination with tacrolimus-loading, inflammation was lower than in control stents used, but still in the range of 1–1.5 inflammation score [33]. However, an increased inflammation score with a remarkably high number of inflammatory cells was observed around the stents in the current study, which was also reflected in a higher fibrin score. Further research is needed to determine whether this is due to the underlying material used (Al/Al<sub>2</sub>O<sub>3</sub> + PTFEP) or whether fractures in the surface coating are to blame.

Finally, SEM imaging was used for the visualization of Al/Al<sub>2</sub>O<sub>3</sub> + PTFEP nanowire coating of explanted stents. SEM pictures showed a specific structure that could be identified as a stent coating. By means of energy dispersive X-Ray spectroscopy the elemental composition of the stent material and the coating were clearly defined and distinguished from each other. EDX analysis approved the SEM results, confirming the presence of Al/Al<sub>2</sub>O<sub>3</sub> + PTFEP in the coating of explanted stents through

elements quantification. While the stent material contained elements from stainless steel, such as chromium, iron and nickel, the coating comprised a high proportion of aluminium and oxygen.

In blood and cell compatibility pre-studies of this study we analysed two-dimensional surfaces [6,12]. However, complete and comprehensive coating of all three-dimensional stent structures and surfaces was challenging and was established under experimental settings. Although all stents underwent light microscopic examination, residual irregular and inhomogeneous coatings are to be expected and may have contributed to the cell reaction in the Al/Al<sub>2</sub>O<sub>3</sub> + PTFEP coated stent group.

## 5. Conclusions

In conclusion, this is the first study in an animal model, which investigated the tolerability and vascular cellular response to a novel nanostructured Al/Al<sub>2</sub>O<sub>3</sub>-coated stent surface with on top PTFEP coating. The placement of these stents in peripheral arteries demonstrated good tolerance without treatment-associated vascular obstruction or thrombus formation and reduced in-stent restenosis on OCT 90 days after implantation. Despite the technical challenges of coating prototypes of Al/Al<sub>2</sub>O<sub>3</sub> + PTFEP coated stents, our results confirm previous cell culture experiments, indicating that the newly super-hydrophobic surface exhibits high cytocompatibility and hemocompatibility with significantly reduced platelet adhesion and activation. However, further improvement of the coating is required, especially to reduce the degree of inflammation in the surrounding tissue. Nonetheless, our findings suggest that PTFEP coating of Al/Al<sub>2</sub>O<sub>3</sub> coated nanowire stents is a promising approach and may have the potential to address in-stent stenosis, a significant challenge in both pediatric and coronary interventional cardiology.

## CRedit authorship contribution statement

**Axel Rentzsch:** Writing – original draft, Visualization, Project administration, Methodology, Investigation, Formal analysis, Data curation. **Eva Metz:** Investigation. **Ruben Mühl-Benninghaus:** Investigation. **Alexander Maßmann:** Methodology, Investigation. **Stephanie Bettink:** Visualization, Investigation. **Bruno Scheller:** Writing – review & editing, Supervision. **Lilia Lemke:** Writing – review & editing, Investigation. **Ali Awadelkareem:** Investigation. **Toshiki Tomori:** Investigation. **Ayman Haidar:** Writing – review & editing, Visualization, Methodology. **Matthias W. Laschke:** Writing – review & editing, Supervision, Project administration, Methodology, Investigation. **Cenk Aktas:** Writing – review & editing, Supervision. **Matthias Hannig:** Writing – review & editing, Supervision. **Norbert Pütz:** Methodology. **Thomas Büttner:** Writing – review & editing, Methodology. **David Scheschkewitz:** Writing – review & editing, Methodology. **Michael Veith:** Supervision, Resources. **Hashim Abdul-Khalik:** Supervision, Investigation, Conceptualization.

## Declaration of competing interest

The following co-authors hold a patent which is related to the contents of the manuscript: Ayman Haidar, Michael Veith, Cenk Aktas, Hashim Abdul-Khalik, Ali Awadelkareem.

Patent title: Beschichtung oder mit einer Beschichtung versehener Körper sowie Verfahren zu deren Herstellung. DAKZ 10 2017 113 7580. 2018; Deutsches Patent- und Markenamt. <https://register.dpma.de/DPMAregister/pat/register?AKZ=1020171137580>.

In addition to this we declare that we have no conflicts of interest to disclose regarding this publication. If any conflicts of interest arise during the course of the publication, we will promptly disclose them to the editor of the publication or to the appropriate parties.

## Acknowledgment

This work was supported by the Gerd Kilian Projektförderung of the Deutsche Herzstiftung.

## Appendix A. Supplementary data

Supplementary data to this article can be found online at <https://doi.org/10.1016/j.carrev.2024.08.017>.

## References

- [1] Hascoet S, Baruteau A, Jalal Z, Mauri L, Acar P, Elbaz M, et al. Stents in paediatric and adult congenital interventional cardiac catheterization. *Arch Cardiovasc Dis.* 2014;107:462–75.
- [2] Russell MR, Blais B, Nia N, Levi DS. The potential impact and timeline of engineering on congenital interventions. *Pediatr Cardiol.* 2020;41:522–38.
- [3] Tomita H, Yazaki S, Kimura K, Ono Y, Yagihara T, Echigo S. Late neointimal proliferation following implantation of stents for relief of pulmonary arterial stenosis. *Cardiol Young.* 2002;12:125–9.
- [4] Inoue T, Croce K, Morooka T, Sakuma M, Node K, Simon DI. Vascular inflammation and repair: implications for re-endothelialization, restenosis, and stent thrombosis. *JACC Cardiovasc Interv.* 2011;4:1057–66.
- [5] Lee KJ, Seto W, Benson L, Chaturvedi RR. Pharmacokinetics of sirolimus-eluting stents implanted in the neonatal arterial duct. *Circ Cardiovasc Interv.* 2015;8.
- [6] Haidar A, Ali AA, Veziroglu S, Fiotowski J, Eichler H, Müller I, et al. PTFEP–Al<sub>2</sub>O<sub>3</sub> hybrid nanowires reducing thrombosis and biofouling. *Nanoscale Adv.* 2019;1:4659–64.
- [7] Veith M, Lee J, Martinez Miro M, Akkan CK, Dufloix C, Aktas OC. Bi-phasic nanostructures for functional applications. *Chem Soc Rev.* 2012;41:5117–30.
- [8] Price RL, Haberstroh KM, Webster TJ. Enhanced functions of osteoblasts on nanostructured surfaces of carbon and alumina. *Med Biol Eng Comput.* 2003;41:372–5.
- [9] Oberringer M, Akman E, Lee J, Metzger W, Akkan CK, Kacar E, et al. Reduced myofibroblast differentiation on femtosecond laser treated 316LS stainless steel. *Mater Sci Eng C Mater Biol Appl.* 2013;33:901–8.
- [10] Aktas OC, Metzger W, Mees L, Martinez MM, Haidar A, Oberringer M, et al. Controlling fibroblast adhesion and proliferation by 1D Al(2)O(3) nanostructures. *IET Nanobiotechnol.* 2019;13:621–5.
- [11] Kiefer K, Lee J, Haidar A, Miro MM, Akkan CK, Veith M, et al. Alignment of human cardiomyocytes on laser patterned biphasic core/shell nanowire assemblies. *Nanotechnology.* 2014;25:495101.
- [12] Kiefer K, Akpınar G, Haidar A, İkier T, Akkan CK, Akman E, et al. Al<sub>2</sub>O<sub>3</sub> micro- and nanostructures affect vascular cell response. *RSC Adv.* 2016;6:17460–9.
- [13] Ali AA, Haidar A, Polonsky O, Faupel F, Abdul-Khaliq H, Veith M, et al. Extreme tuning of wetting on 1D nanostructures: from a superhydrophilic to a perfect hydrophobic surface. *Nanoscale.* 2017;9:14814–9.
- [14] Haidar A, Veith M, Aktas C, Abdul-Khaliq H, Awadelkareem AA. Beschichtung oder mit einer Beschichtung versehener Körper sowie Verfahren zu deren Herstellung. DAKZ 10 2017 113 7580 Deutsches Patent- und Markenamt; 2018 <https://register.dpma.de/DPMAregister/pat/register?AKZ=1020171137580>.
- [15] Schwartz RS, Edelman E, Virmani R, Carter A, Granada JF, Kaluza GL, et al. Drug-eluting stents in preclinical studies: updated consensus recommendations for preclinical evaluation. *Circ Cardiovasc Interv.* 2008;1:143–53.
- [16] Moreno PR, Palacios IF, Leon MN, Rhodes J, Fuster V, Fallon JT. Histopathologic comparison of human coronary in-stent and post-balloon angioplasty restenotic tissue. *Am J Cardiol.* 1999;84(462–466):a469.
- [17] Templin C, Meyer M, Müller MF, Djonov V, Hlushchuk R, Dimova I, et al. Coronary optical frequency domain imaging (OFDI) for in vivo evaluation of stent healing: comparison with light and electron microscopy. *Eur Heart J.* 2010;31:1792–801.
- [18] Murata A, Wallace-Bradley D, Tellez A, Alviar C, Aboodi M, Sheehy A, et al. Accuracy of optical coherence tomography in the evaluation of neointimal coverage after stent implantation. *JACC Cardiovasc Imaging.* 2010;3:76–84.
- [19] Okamura T, Gonzalo N, Gutiérrez-Chico JL, Serruys PW, Bruining N, de Winter S, et al. Reproducibility of coronary Fourier domain optical coherence tomography: quantitative analysis of in vivo stented coronary arteries using three different software packages. *EuroIntervention.* 2010;6:371–9.
- [20] Lemos PA, Takimura CK, Laurindo FR, Gutierrez PS, Aiello VD. A histopathological comparison of different definitions for quantifying in-stent neointimal tissue: implications for the validity of intracoronary ultrasound and optical coherence tomography measurements. *Cardiovasc Diagn Ther.* 2011;1:3–10.
- [21] Aktas C, Dörrschuck E, Schuh C, Miró MM, Lee J, Pütz N, et al. Micro- and nanostructured Al<sub>2</sub>O<sub>3</sub> surfaces for controlled vascular endothelial and smooth muscle cell adhesion and proliferation. *Mater Sci Eng C.* 2012;32:1017–24.
- [22] Bedair TM, Min IJ, Park W, Joung YK, Han DK. Sustained drug release using cobalt oxide nanowires for the preparation of polymer-free drug-eluting stents. *J Biomater Appl.* 2018;33:352–62.
- [23] Aggarwal V, Dhillon GS, Penny DJ, Gowda ST, Qureshi AM. Drug-eluting stents compared with bare metal stents for stenting the ductus arteriosus in infants with ductal-dependent pulmonary blood flow. *Am J Cardiol.* 2019;124:952–9.
- [24] Lipinski MJ, Forrestal BJ, Iantorno M, Torguson R, Waksman R. A comparison of the ultrathin Orsiro hybrid sirolimus-eluting stent with contemporary drug-eluting stents: a meta-analysis of randomized controlled trials. *Cardiovasc Revasc Med.* 2018;19:5–11.
- [25] Iglesias JF, Roffi M, Losdat S, Muller O, Degrauwe S, Kurz DJ, et al. Long-term outcomes with biodegradable polymer sirolimus-eluting stents versus durable polymer everolimus-eluting stents in ST-segment elevation myocardial infarction: 5-year follow-up of the BIOSSTEMI randomised superiority trial. *Lancet.* 2023;402:1979–90.
- [26] Iglesias JF, Roffi M, Degrauwe S, Secco GG, Aminian A, Windecker S, et al. Orsiro cobalt-chromium sirolimus-eluting stent: present and future perspectives. *Expert Rev Med Devices.* 2017;14:773–88.
- [27] Nuhn H, Blanco CE, Desai TA. Nanoengineered stent surface to reduce in-stent restenosis in vivo. *ACS Appl Mater Interfaces.* 2017;9:19677–86.
- [28] Henn C, Satz S, Christoph P, Kurz P, Radeleff B, Stampfl U, et al. Efficacy of a polyphosphazene nanocoat in reducing thrombogenicity, in-stent stenosis, and inflammatory response in porcine renal and iliac artery stents. *J Vasc Interv Radiol.* 2008;19:427–37.
- [29] Cutlip DE, Garratt KN, Novack V, Barakat M, Meraj P, Maillard L, et al. 9-month clinical and angiographic outcomes of the COBRA Polyene-F NanoCoated coronary stent system. *JACC Cardiovasc Interv.* 2017;10:160–7.
- [30] Mori H, Jinnouchi H, Diljon C, Torii S, Sakamoto A, Kolodgie FD, et al. A new category stent with novel polyphosphazene surface modification. *Future Cardiol.* 2018;14:225–35.
- [31] Scheller B, Kuhler M, Cremers B, Mahnkopf D, Bohm M, Boxberger M. Short- and long-term effects of a novel paclitaxel coated stent in the porcine coronary model. *Clin Res Cardiol.* 2008;97:118–23.
- [32] Kollum M, Farb A, Schreiber R, Terfera K, Arab A, Geist A, et al. Particle debris from a nanoporous stent coating obscures potential antiproliferative effects of tacrolimus-eluting stents in a porcine model of restenosis. *Catheter Cardiovasc Interv: official journal of the Society for Cardiac Angiography & Interventions.* 2005;64:85–90.
- [33] Wieneke H, Dirsch O, Sawitowski T, Gu YL, Brauer H, Dahmen U, et al. Synergistic effects of a novel nanoporous stent coating and tacrolimus on intima proliferation in rabbits. *Catheter Cardiovasc Interv: official journal of the Society for Cardiac Angiography & Interventions.* 2003;60:399–407.